

## Neutron-diffraction study of the staggered magnetization of $\text{CuCl}_2 \cdot 2\text{D}_2\text{O}$

J. W. Lynn

*Department of Physics, Brookhaven National Laboratory,\* Upton, New York 11973  
and Department of Physics, University of Maryland, † College Park, Maryland 20742*

P. Heller

*Department of Physics, Brandeis University, ‡ Waltham, Massachusetts 02154*

N. A. Lurie<sup>§</sup>

*Department of Physics, Brookhaven National Laboratory,\* Upton, New York 11973  
and Department of Physics, Brandeis University, ‡ Waltham, Massachusetts 02154*

(Received 18 July 1977)

The neutron-scattering technique has been used to measure the staggered magnetization of the  $S = 1/2$ ,  $d = 3$  antiferromagnet  $\text{CuCl}_2 \cdot 2\text{D}_2\text{O}$  as a function of temperature and magnetic field. The critical exponents  $\beta_1$ ,  $\beta_2$  describing the temperature variation of the order parameter in the regions well above and well below the bicritical point, respectively, were found to be  $\beta_1 = 0.321 \pm 0.01$  and  $\beta_2 = 0.324 \pm 0.013$ . These values are within experimental error of the theoretically expected value of 0.325 for the  $d = 3$  Ising model. At the spin-flop transition the staggered magnetization changed 8% in magnitude, the reduction being due to the anisotropy of the  $g$  factor. The magnetic form factor in the spin-flop region was found to be the same as that previously determined in zero field. In addition, with the applied field tilted in the  $a$ - $b$  plane away from the  $\vec{a}$  axis, the direction of the staggered magnetization was found to rotate continuously from the  $\vec{a}$  to the  $\vec{b}$  direction as is expected theoretically. The observed range in field over which the rotation takes place, however, is narrower than the predictions of mean-field theory.

### I. INTRODUCTION

Antiferromagnets exhibiting field-induced transitions can roughly be divided into two classes depending on whether the isotropic or the anisotropic interactions are predominant. The first class typically exhibits spin flopping and bicritical points in the (axial) field-temperature plane. The second class of materials provides us with examples of metamagnetic and tricritical behavior. Although the former class was the first to be investigated, there are essentially no quantitative experimental studies which provide microscopic information on the details of the ordering at the field-induced transitions in these systems.

Historically the system in which the phenomenon of spin flopping predicted by Néel<sup>1</sup> was first observed<sup>2, 3</sup> is  $\text{CuCl}_2 \cdot 2\text{H}_2\text{O}$ , which requires only a modest applied field for its study. This now well known spin-flop effect may be described briefly as follows: When the strength of a magnetic field applied exactly along the easy magnetic axis<sup>4</sup> ( $\vec{a}$  axis) is increased from zero, a spin-reorientation critical field  $H_{\text{SF}}$  is encountered in which the direction of the moments on the two sublattices abruptly "flop" from their antiferromagnetic (AF) configuration (parallel and antiparallel along the  $\vec{a}$  axis) to a new spin-flopped (SF) configuration in which the basic antiferromagnetic arrangement is along the next-easiest ( $\vec{b}$ ) magnetic axis. In

addition there is a small induced ferromagnetic component along the  $\vec{a}$  axis described by the angle  $\theta$ , shown schematically in Fig. 1. With further field increase  $\theta$  increases and at sufficiently high fields ( $\sim 150$  kOe for  $\text{CuCl}_2 \cdot 2\text{H}_2\text{O}$ )<sup>5</sup> a second-order phase boundary to the paramagnetic (P) phase is approached as  $\theta$  approaches  $90^\circ$ . A portion of the phase diagram for  $\text{CuCl}_2 \cdot 2\text{D}_2\text{O}$  is shown in Fig. 1. The data points are those obtained in the present experiments, and are very close to those obtained by Butterworth and Zidell<sup>6</sup> for the isomorphic hydrated system. We have not, however, attempted to make a detailed mapping of the phase diagram. We have chosen to deuterate our sample to avoid the large incoherent scattering cross sections associated with hydrogen, and thus improve the quality of our data.

The nature of the various transitions between the AF, SF, and P phases is best described in terms of the vectorial staggered magnetization defined by

$$\vec{M}_{\text{stag}} = \frac{1}{2} (\langle \vec{M}_{\text{subl}1} \rangle - \langle \vec{M}_{\text{subl}2} \rangle). \quad (1)$$

This order parameter can be conveniently pictured as one-half the vector<sup>7</sup> joining the tips of the arrows in Fig. 1. Then for  $H < H_{\text{SF}}$ ,  $\vec{M}_{\text{stag}}$  is along  $\vec{a}$ , while for  $H > H_{\text{SF}}$ ,  $\vec{M}_{\text{stag}}$  is along  $\vec{b}$ , and the boundary separating these two phases is clearly a line of first-order phase transitions.

If we now vary the temperature at a fixed  $H < H_{\text{SF}}$ , then we approach the AF-P phase boundary as de-

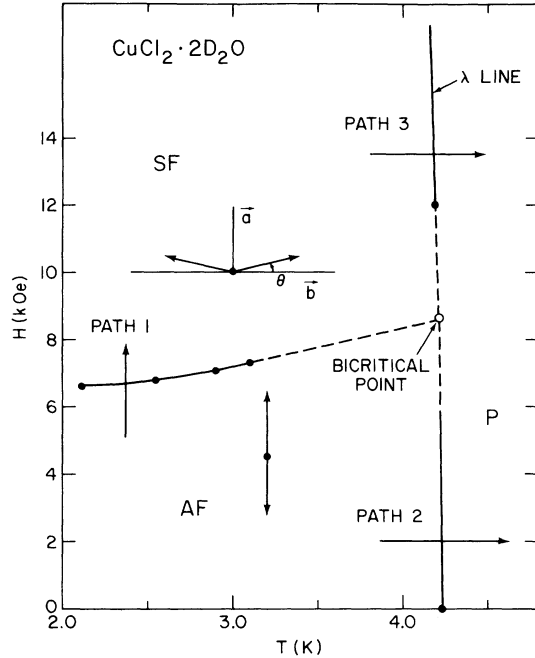


FIG. 1. Magnetic phase diagram for  $\text{CuCl}_2 \cdot 2\text{D}_2\text{O}$  in the  $H$ - $T$  plane, showing the antiferromagnetic (AF), spin-flop (SF), and paramagnetic (P) regions. The intersection of the first-order spin-flop line with the second-order  $\lambda$  lines is the bicritical point.

picted by path 2. This boundary is a line of second-order critical points, with the direction of the staggered magnetization remaining along  $\hat{a}$  and its magnitude decreasing continuously to zero with a power-law behavior:

$$\vec{M}_{\text{stag}} \propto \hat{a} [T_{\parallel}(H) - T]^{\beta_{\parallel}}. \quad (2)$$

Here  $T_{\parallel}(H)$  is the AF-P phase boundary temperature at field  $H$  and  $\beta_{\parallel}$  is the critical exponent describing the temperature variation of the long-range order parameter along the (unit) vector direction  $\hat{a}$ . Analogously, for  $H > H_{\text{SF}}$  we follow path 3, and  $\vec{M}_{\text{stag}}$  is given by

$$\vec{M}_{\text{stag}} \propto \hat{b} [T_{\perp}(H) - T]^{\beta_{\perp}}, \quad (3)$$

where  $\vec{M}_{\text{stag}}$  remains along the (unit) vector  $\hat{b}$ .

For each of these second-order  $\lambda$  lines only a single component of the order parameter shows a critical divergence as the phase boundary is approached. This is because the divergent critical fluctuations occur only in the components of the staggered magnetization which have nonvanishing values in the ordered phase. An exception to this occurs at the bicritical point,<sup>8</sup> which is the intersection of the SF-P and AF-P lines. Here two components have divergent fluctuations simultaneously. Elsewhere  $\vec{M}_{\text{stag}}$  is restricted to a unique

axis and therefore the dimensionality  $n$  of the order parameter is one. In addition, on the basis of universality<sup>9</sup> one would expect the exponents  $\beta_{\parallel}$  and  $\beta_{\perp}$  to be field independent along their respective  $\lambda$  lines. With the spatial dimensionality  $d=3$ , we thus expect (for  $H \neq H_{\text{SF}}$ ) both transitions to be described by three-dimensional Ising exponents, viz.,<sup>10</sup>

$$\beta_{\parallel} = \beta_{\perp} = \beta_{\text{Ising}} = 0.325. \quad (4)$$

Our initial interest was thus concerned with using the neutron-scattering technique to examine the validity of (4) for both transitions.

The situation is much more complicated when the applied field is not directed along the easy axis. Generally a first-order phase transition to the flopped state is *not* expected theoretically, the vector  $\vec{M}_{\text{stag}}$  instead undergoing a continuous rotation from the vicinity of  $\hat{a}$  to the vicinity of  $\hat{b}$  as the field strength is increased.<sup>11, 12</sup> For a first-order SF transition, the angle  $\psi$  between the easy axis and the (projection in the  $a$ - $b$  plane of the) field  $\vec{H}$  must be smaller than a critical value<sup>11</sup>  $\psi_c$  of the order of a few tenths of a degree. For  $|\psi| > \psi_c$ ,  $\vec{M}_{\text{stag}}$  rotates continuously, a curve of rotation angle versus field strength becoming infinitely steep as  $|\psi| \rightarrow \psi_c$ . The corresponding critical lines<sup>13</sup> in the temperature-field space<sup>14</sup> correspond to the edges of the "shelf" of first-order flop transitions.<sup>15</sup>

The angular orientational behavior of  $\vec{M}_{\text{stag}}$  in the vicinity of the SF transition is thus also of fundamental interest. Since the neutron-scattering cross section is sensitive to the orientation of the magnetic moments, this behavior is directly measurable. We report here a rather preliminary experiment of this kind; a proper study obviously would require an extremely homogeneous field and narrow sample mosaic spread. Since these conditions were not met, we confined our studies of the angular behavior to the case of substantial applied field misalignment. By the same token, in studying the SF-P and AF-P critical behaviors for the case of  $\vec{H}$  nominally along  $\hat{a}$ , we avoided the region around the bicritical point where precise alignment is important. Thus we did not attempt to study the bicritical behavior, and in particular to examine the effect of crossover from  $n=1$  to  $n=2$  at the bicritical point. This crossover will be particularly interesting to observe but would require, in addition to the conditions just mentioned, temperature control better than was available to us. Such studies will be relegated to the future and the present work should thus be regarded as a first step toward a study of the spin-flop and related transitions using a microscopic probe.

## II. EXPERIMENTAL TECHNIQUES

### A. Structure and cross section

The crystal structure<sup>16</sup> of copper chloride dideuterate (and its hydrated isomorph) is orthorhombic with space group  $D_{2h}^7$  ( $Pbmn$ ). The magnetic  $\text{Cu}^{2+}$  ions occupy the centered positions in the  $a$ - $b$  faces and the corner positions of the unit cell. In the zero-field ordered magnetic state the moments in each  $a$ - $b$  plane are oriented parallel to each other, while the moments in adjacent  $a$ - $b$  planes are antiparallel to each other.<sup>17</sup> Thus the magnetic unit cell is twice the chemical unit cell along the  $c$  axis, and the magnetic-reciprocal-lattice positions  $(h, k, l)$ , referred to the chemical unit cell,<sup>18</sup> occur at  $h+k$  even integer,  $h, k$  integers,  $l$  half integer. In addition to this basic spin configuration there is a small antiferromagnetic canting of the moments<sup>19</sup> out of the  $a$ - $b$  plane caused by the antisymmetric exchange interaction,<sup>20</sup> but here we are not concerned with this component and therefore have not included it in the discussion or the analysis.

The intensity of the magnetic Bragg peaks is given by<sup>21</sup>

$$I(\vec{\tau}) \propto |f(\vec{\tau})|^2 \left| \sum_{\vec{R}_j} e^{i\vec{\tau} \cdot \vec{R}_j} \{ \vec{\tau} \times (\vec{M}_j \times \vec{\tau}) \} \right|^2 \quad (5a)$$

$$= |f(\vec{\tau})|^2 \left| \sum_{\vec{R}_j} e^{i\vec{\tau} \cdot \vec{R}_j} \{ \vec{M}_j^\perp \} \right|^2, \quad (5b)$$

where  $f(\vec{\tau})$  is the atomic magnetic form factor,  $\hat{\tau}$  is a unit vector in the direction of the magnetic reciprocal lattice vector  $\vec{\tau}$ ,  $\vec{M}_j$  is the magnetic moment at the site  $j$ , and the sum is over all positions  $\vec{R}_j$  of the magnetic ions in the magnetic unit cell.  $\vec{M}_j^\perp$  is defined in going from Eq. (5a) to (5b) and is the projection of the vector  $\vec{M}_j$  on the plane perpendicular to  $\hat{\tau}$ . For the magnetic structure<sup>17</sup> of  $\text{CuCl}_2 \cdot 2\text{D}_2\text{O}$  Eq. (5b) reduces to

$$I(\vec{\tau}) \propto |f(\vec{\tau})|^2 |\vec{M}_{\text{stag}}^\perp|^2. \quad (5c)$$

Under the conditions of our experiment, in which  $\vec{M}_{\text{stag}}$  was in the  $a$ - $b$  plane and  $\vec{\tau}$  restricted to the  $(0, k, l)$  scattering plane, we have finally

$$I(\vec{\tau}) \propto |f(\vec{\tau})|^2 |\vec{M}_{\text{stag}}|^2 (1 - \tau_b^2 \sin^2 \phi), \quad (6)$$

where  $\phi$  is the angle between  $\vec{M}_{\text{stag}}$  and  $\hat{a}$ , and

$$\tau_b = \hat{\tau} \cdot \hat{b} = (k/b) [(k/b)^2 + (l/c)^2]^{-1/2}. \quad (7)$$

If  $\vec{H} \parallel \hat{a}$ , this simplifies to

$$I(\vec{\tau}) \propto \begin{cases} |f(\vec{\tau})|^2 |\vec{M}_{\text{stag}}|^2, & H < H_{\text{SF}}; \vec{M}_{\text{stag}} \parallel \hat{a} \\ |f(\vec{\tau})|^2 |\vec{M}_{\text{stag}}|^2 \tau_c^2, & H > H_{\text{SF}}; \vec{M}_{\text{stag}} \parallel \hat{b}, \end{cases} \quad (8)$$

where  $\tau_c$  is the component of the unit vector  $\hat{\tau}$  along the  $c$  axis. Here the staggered magnetization<sup>7</sup> is related to the atomic magnetic moments by

$$\vec{M}_{\text{stag}} = \frac{1}{2} g_a \mu_B \hat{a} (\langle S_1^a \rangle - \langle S_2^a \rangle), \quad H < H_{\text{SF}}, \quad (9a)$$

$$\vec{M}_{\text{stag}} = g_b \mu_B \cos \theta \hat{b} |\langle \vec{S}_{1\text{or}2} \rangle|, \quad H > H_{\text{SF}}, \quad (9b)$$

where  $\langle S \rangle$  is the thermal average of the spin at temperature  $T$  and field  $H$ ,  $g_a$  and  $g_b$  are the spectroscopic splitting factors appropriate for the  $\hat{a}$  and  $\hat{b}$  axes, respectively, and  $\theta$  is the angle between the moment and the  $\hat{b}$  axis in the flopped phase as shown in Fig. 1. It is clear that in the SF phase the intensity is proportional only to the component of the moments along the  $\hat{b}$  axis, that is, to the staggered magnetization. The components parallel to  $\hat{a}$  give rise to new independent magnetic-reciprocal-lattice points which occur at the same  $(h, k, l)$  as the nuclear peaks (analogous to a ferromagnet). They are of no interest in the present study.

Equations (6), (8), and (9) have been used to interpret all of our data. The important point is that the observed Bragg intensities at these magnetic-reciprocal-lattice points are directly related to the staggered magnetization. For example, in the particular case of the AF-SF transition (path 1) the intensity at each reciprocal-lattice point must satisfy

$$\frac{I_{\text{SF}}}{I_{\text{AF}}} = \frac{|M_{\text{stag}}^{\text{SF}}|^2}{|M_{\text{stag}}^{\text{AF}}|^2} (1 - \tau_b^2), \quad (10)$$

which yields directly the field dependence of  $\vec{M}_{\text{stag}}$ . In the more general case of  $\vec{H}$  not parallel to  $\hat{a}$  the temperature and field dependence of these intensities can be used to obtain not only the magnitude of  $\vec{M}_{\text{stag}}$ , but its *direction* as well.

### B. Data collection

The single crystal of  $\text{CuCl}_2 \cdot 2\text{D}_2\text{O}$  used for the present measurements was the same crystal used by Umebayashi *et al.*<sup>19</sup> in their study of the spin density. Some deterioration of the surface of the crystal had occurred, so the volume of the crystal was reduced to  $\sim 25 \text{ mm}^3$ . The crystal was sealed in an Al container with a helium atmosphere and then mounted in a cold-finger liquid-helium cryostat. The required temperatures were attained by pumping on the helium bath until the temperature of the sample was just below the desired value, and then controlling the temperature at the set point with an electrical heater. The temperature was measured with a calibrated Ge sensor imbedded in the pedestal near the sample and then was controlled by an ac bridge and servo control arrangement. The control was better than 0.3 mK over a 30-min period and better than 1 mK over a 24-h period. For the case when the magnetic field was applied, the magnetoresistance of the Ge sensor was taken into account by comparing the read-

ing with a calibrated GaAs sensor, and also by directly observing the change in the resistance of the Ge sensor over a short period of time when the field was turned on and off. At the fields used this changed the apparent temperature from the  $H=0$  value by  $\sim 7$  mK. More importantly, the change in the slope of the resistance vs temperature curve near the phase transition, which would affect the value of the critical exponents obtained from the data, was small.

A conventional iron-core magnet was used to produce the external magnetic field. To provide a vertical field, an axial hole was drilled in the top pole piece to allow entry of the cryostat tail section. The cryostat itself was mounted on top of the magnet and was constructed so as to allow the tilts of the cryostat and magnet to be independently adjusted in a range of  $\pm 4^\circ$ . Thus the crystal could be aligned so that the  $(0, k, l)$  scattering plane was maintained while the magnetic field was adjusted with respect to the  $\hat{a}$  axis. Of course, the hole in the pole piece produced a considerable inhomogeneity in the magnetic field, of the order of 30 Oe at  $\sim 8$  kOe both horizontally and vertically. This is not significant for the measurements of the critical exponents in the present case, but would preclude any measurements in the vicinity of the bicritical point. The time stability of the current supply was better than 1 part in  $10^5$ .

The experiments were performed at the Brookhaven high flux beam reactor. Initially a two-axis crystal spectrometer was used to measure the integrated Bragg intensities of several reflections as a function of temperature. These measurements served primarily to establish that the magnetic reflections of interest were free of extinction effects<sup>22</sup> and also of multiple and parasitic Bragg reflections. The incident wavelength in all our measurements was chosen to be  $2.35 \text{ \AA}$  so that pyrolytic graphite filters could be used to eliminate (better than  $10^{-6}$  reduction) higher-order wavelengths in the incident beam.

To increase instrumental resolution and at the same time discriminate against inelastic scattering processes, a triple-axis spectrometer was used to measure the magnetic Bragg intensities. This yielded a signal-to-noise ratio of 800:1 at low temperatures ( $\sim 2.0$  K) of 800:1 for the strongest magnetic Bragg peak [the  $(0, 0, \frac{1}{2})$ ]. This was 10 times better than with the two-axis spectrometer, a very important improvement for studying the behavior near the ordering temperature. In addition, the triple-axis technique helps discriminate against the magnetic critical scattering, which is the factor in the present experiment which limits how close to the transition the order parameter can be reliably determined. In order to improve

on the present data, accurate measurements of the critical scattering would have to be made. In the results presently reported the measurements of the order parameter were limited to 4 mK of the transition temperature due to both the critical scattering and the temperature resolution.

### III. RESULTS AND INTERPRETATION

#### A. Spin-flop transition

In Fig. 2 we plot the intensity of the  $(0, 2, \frac{3}{2})$  magnetic reflection as a function of the applied field strength. This has been done for field directions corresponding to misalignments in the  $a$ - $b$  plane of  $\psi = 0^\circ, 2^\circ,$  and  $4^\circ$  from the easy axis.<sup>23</sup> In each case the intensity decreases by a factor of  $0.60 \pm 0.03$  in going from the AF to the flopped state. Since  $1 - \tau_b^2 = 0.725$ , we find from Eq. (10) that

$$|\vec{M}_{\text{stag}}|_{\text{SF}}^2 / |\vec{M}_{\text{stag}}|_{\text{AF}}^2 = 0.83 \pm 0.04. \quad (11)$$

This result was confirmed for the  $(0, 0, \frac{1}{2})$  reflection: In this case, where  $\tau_b = 0$ , the intensity decreased by a factor of 0.85. In attributing these reductions to a drop in  $|\vec{M}_{\text{stag}}|^2$ , we are assuming that the magnetic form factor is unaffected by the

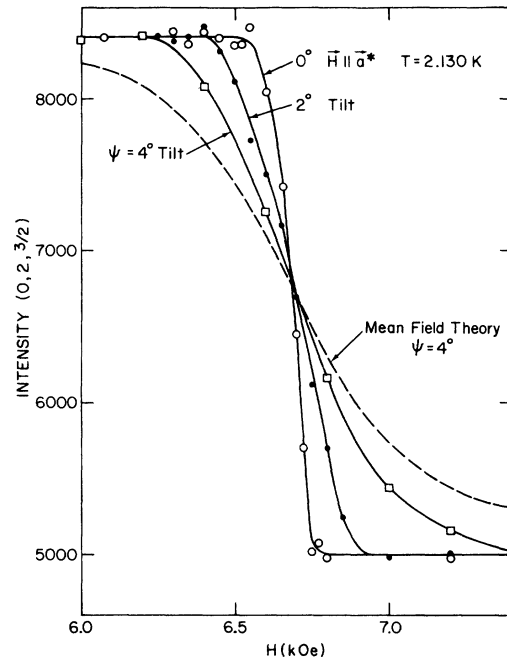


FIG. 2. Intensity of the  $(0, 2, \frac{3}{2})$  magnetic peak as a function of applied magnetic field, showing the intensity change at the spin-flop transition. The curves labeled  $0^\circ, 2^\circ$  and  $4^\circ$  tilt refer to the angle of the magnetic field with respect to the crystallographic  $a$  axis. The solid curves through those data are guides to the eye. The dashed curve is the result of the molecular field calculations as discussed in the text.

field. To check this, we measured a series of peaks, finding that the intensities in the SF state were consistent with Eq. (8) using the form factor determined in zero field,<sup>19</sup> there being a constant reduction with respect to the AF intensities at all reflections. Thus there is no substantial change in the magnetic form factor due to the spin-flop transition, as has already been noted.<sup>24</sup> Consequently the intensity changes must be due to a change in  $|\vec{M}_{\text{stag}}|$ , and in comparing Eq. (9a) to (9b), this change could be attributed to a change in  $\langle S \rangle$ ,  $g$ , or the angle  $\theta$ . At first thought one might assign this result to  $\theta$ . But this would require  $\theta$  to be  $23^\circ$ , with a corresponding  $\vec{a}$ -axis moment of  $0.40 \mu_B/\text{ion}$  just above the SF line. This is very much larger than expected on the basis of an upper critical field<sup>5</sup> of  $\sim 150$  kOe, from which mean-field theory would predict  $\theta = \sin^{-1}(6.7/150) \cong 2.6^\circ$ . The calculated reduction in  $|\vec{M}_{\text{stag}}|^2$ , which is only second order in  $\theta$ , would then be 0.998. This is clearly at variance with our data. Here we are assuming, as we think is surely true at these temperatures, that the individual sublattice spins are essentially saturated. Then the observed intensity ratio must be due to the anisotropy of the  $g$  factor. Indeed Van den Handel *et al.*<sup>25</sup> found from susceptibility measurements that the saturated moments along the  $a$  and  $b$  axes were  $1.10$  and  $1.01 \mu_B$  per spin, respectively. This would give an intensity ratio of 0.84, in good agreement with our observations.

We next consider the shape and width of the experimental curves of Fig. 2. In no case was an abrupt jump in intensity detected. This is not surprising in view of the very narrow angular width ( $\psi_c \sim 0.1^\circ$ ) expected theoretically for the shelf of first-order spin-flop transitions. For the magnet we used, the (axial) inhomogeneity in the field strength over the sample was  $\sim 30$  Oe, and the directional inhomogeneity over the size of the sample was  $\pm 0.3^\circ$ . Hence the experimental curves must be a composite of differing curves, most of which do not even exhibit a first-order discontinuity. In this light the experimental curve for the nominally aligned case ( $\psi = 0^\circ$ ) is quite understandable.

Despite this we can actually draw a rather interesting conclusion from the curve corresponding to the data taken with the substantial misalignment of  $\psi = 4^\circ$ . This curve is actually appreciably narrower than we would infer from the mean-field theory of Refs. 11 and 12. Our reasoning here is as follows: In the mean-field theory (at  $T = 0^\circ\text{K}$ ) the angular width  $\psi_c$  of the spin-flop transition is determined by the intrasublattice ( $-K_2$ ) ( $a$ - $b$  plane) anisotropy energy, while the spin-flop field is determined by the sum ( $K_1 - K_2$ ) of the intersublattice and intrasublattice anisotropies. Adopting the results of Refs. 11 and 12 for the  $S = \frac{1}{2}$  case, we find

$$\tan\psi_c = \left| \frac{H_{\text{SF}}(T=0)}{H_{\text{SF-P}}(T=0)} \right|^2 \frac{(-K_2)}{K_1 - K_2}. \quad (12)$$

This gives  $\psi_c \approx 0.11^\circ$  assuming that  $|K_2|$  is comparable with  $|K_1 - K_2|$ . Thus for  $\psi = 4^\circ$ , we are well outside the region of the first-order shelf of spin-flop transitions, i.e.,

$$\psi \gg \psi_c. \quad (13)$$

When this condition is satisfied we find by following the numerical free-energy minimization procedures outlined in Ref. 12 that the way in which the vector  $\vec{M}_{\text{stag}}$  rotates from near  $\hat{a}$  to near  $\hat{b}$  as the field strength is increased is essentially independent of the ratio of the inter- and intrasublattice anisotropies for a given value of the flop field. Moreover, when (13) holds, the mean-field description of the turning of  $\vec{M}_{\text{stag}}$  reduces essentially to the expression

$$\tan[2(\phi + \psi)] = \frac{\sin 2\psi}{\cos 2\psi - (H/H_{\text{SF}})^2}. \quad (14)$$

Here  $\psi$  is the misalignment of the field in the  $a$ - $b$  plane from the easy axis (taken, say, in the clockwise sense) while  $\phi$  is the corresponding misalignment of  $\vec{M}_{\text{stag}}$  (taken, then in the counterclockwise sense). The simple expression (14) has a long history<sup>26-28</sup> going all the way back to Néel.<sup>1</sup> It is interesting to note that its derivation contained approximations that prevented the essential physics of the SF shelf-edge transitions from appearing. This physics does appear in the correct mean-field description<sup>11, 12</sup> and as Rohrer<sup>15</sup> has recently shown, in nature. Equation (14) is nonetheless the essential mean-field result when  $\psi \gg \psi_c$ .

Thus, using either the numerical mean-field techniques of Refs. 11 and 12, or Eq. (14), (suitably modified<sup>28</sup> for the slight  $g$ -factor anisotropy) we computed the intensity of the  $(0, 2, \frac{3}{2})$  reflection for  $\psi = 4.0^\circ$  as a function of  $H$ . This could be done unambiguously since the known value of the flop field is the only parameter which substantially affects the calculation. The result is indicated in Fig. 2 by the dashed curve. This is considerably broader than the corresponding experimental curve, a result<sup>29</sup> which is surely not an artifact of the field inhomogeneity.

#### B. SF-P and AF-P transitions

The curves of Fig. 2 showed that the width of the continuous spin-flop "transition" is a rather sensitive measure of the field alignment. We are thus confident that the nominal  $\vec{a}$ -axis position was correct to within  $\pm \frac{1}{4}^\circ$ . Although this alignment would be far too crude for studying the bicritical behavior, it should be more than adequate for studying

the SF-P transition at a field well above the bicritical field,  $H_b \approx 8.5$  kOe. Thus for the measurements along path 3 we chose to work at  $H = 12.0$  kOe. For this separation from the bicritical field mean-field calculations showed no trace of the effect of a possible  $\frac{1}{2}^\circ$  misalignment on the computed Bragg intensities.

We first describe our method of analysis for this SF-P case. Our results for the intensity of the  $(0, 0, \frac{1}{2})$  magnetic reflection at  $H = 12$  kOe are shown in Fig. 3 from just below  $T = 2^\circ\text{K}$ , the lowest temperature studied, up through the critical region. The expanded scale on the right-hand side accentuates the data near the transition temperature. Recall that the Bragg intensity is proportional to  $|\vec{M}_{\text{stag}}|^2$ , which should decrease continuously to zero, (remaining concave-down if  $\beta < \frac{1}{2}$ ). The small rounding near the transition is due to magnetic critical scattering. A temperature-independent background is also evident.

In the critical region the magnitude of the staggered magnetization can be written

$$|\vec{M}_{\text{stag}}| = |\vec{M}_{\text{stag}}(0)| B_{\parallel, \perp} [(T_{\parallel, \perp} - T)/T_{\parallel, \perp}]^{\beta_{\parallel, \perp}}, \quad (15)$$

where the subscripts  $\parallel$  and  $\perp$  refer, respectively, to the AF-P and SF-P cases. We anticipate that the square of this relation will describe the Bragg component of the observed intensity; the critical

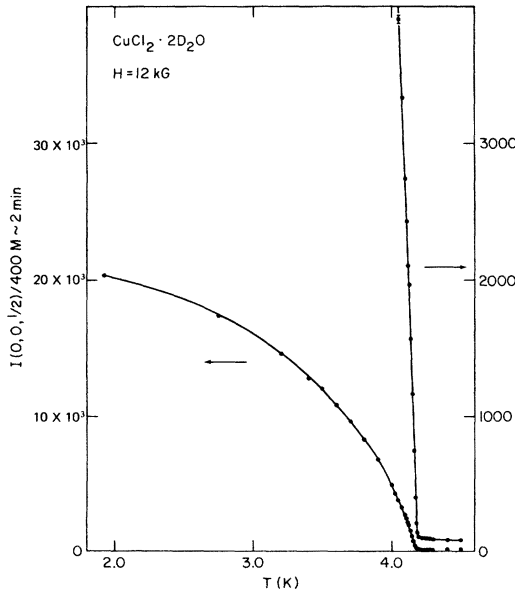


FIG. 3. Intensity of the  $(0, 0, \frac{1}{2})$  reflection as a function of temperature. The applied field is 12 kOe, so  $H > H_{\text{SF}}$ .  $M$  is the incident-neutron-beam monitor.

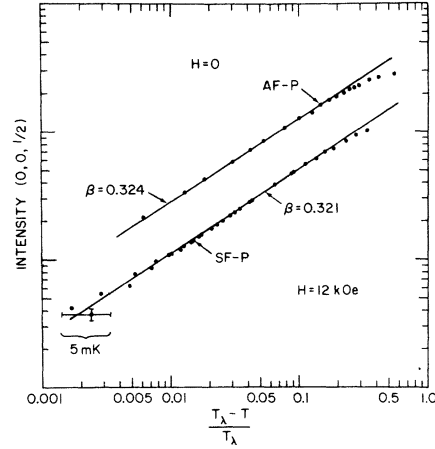


FIG. 4. Intensity vs reduced temperature data for  $H=0$  and  $H=12$  kOe. The solid curves are the least-squares fits to the data as discussed in the text.  $T_\lambda$  refers to the critical temperature at the field  $H$ .

scattering component consists of a weak superimposed peak which is roughly symmetric about the transition temperature. Then, since  $\beta < \frac{1}{2}$ , the observed curve should in principle have an infinite slope at the transition temperature and only there. Since the critical scattering was small, we first neglected it, except that we deleted the data points which appeared to be affected. We then least-squares fitted the observed intensity, corrected for background, to

$$I_{\text{obs, corr}} = I_{\text{obs, corr}}(0) B_\perp^2 [(T_\perp - T)/T_\perp]^{2\beta_\perp},$$

allowing  $B_\perp$ ,  $\beta_\perp$ , and  $T_\perp$  to vary independently. As a check on the transition temperature, we located the point of maximum slope of the raw intensity versus temperature curve. This transition temperature agreed to within the statistical uncertainty with the value found in the least-squares fit.

An exactly analogous technique was employed to analyze the case of the AF-P transition. We did this in zero field (path 2 with  $H=0$ ). The raw data (not shown) are very similar to those of Fig. 3. The data and the fitted functions for both cases are shown in Fig. 4. The results of the fits are

$$\beta_\perp = 0.321 \pm 0.01, \quad T_\perp = 4.196 \pm 0.004$$

for the SF-P transition at  $H=12$  kOe, and

$$\beta_\parallel = 0.324 \pm 0.013, \quad T_\parallel = 4.225 \pm 0.01$$

for the AF-P transition at  $H=0$ . The quoted errors are considered to represent three standard deviations. The (nonuniversal) amplitude  $B$  was  $1.4 \pm 0.1$  in both cases, the rather large error being due to the uncertainties in  $I_{\text{obs}}(0)$ , which was

estimated by extrapolating the raw data to  $T = 0$ .

Because of the critical scattering and other experimental difficulties discussed in Sec. II, our results are limited to reduced temperatures  $t = (T_{\parallel, \perp} - T)/T_{\parallel, \perp}$  greater than  $2 \times 10^{-3}$ , the range of the least-square fits being  $2 \times 10^{-3} < t < 1.4 \times 10^{-1}$  for the SF-P data and  $5 \times 10^{-3} < t < 2.2 \times 10^{-1}$  for the AF-P. For the latter case our results are in good agreement with the NMR results of Ref. 2, although we found no evidence for the exponent crossover which had been inferred by one of us (P.H.) from the NMR data<sup>30</sup> closer to the transition.

#### IV. CONCLUSIONS

The  $d=3$  Ising-like character expected theoretically at the spin-flop to paramagnetic phase transition in the orthorhombic antiferromagnet  $\text{CuCl}_2 \cdot 2\text{D}_2\text{O}$  has been confirmed experimentally by using neutron scattering to probe the temperature dependence of the transverse staggered magnetization at a fixed field well above the bicritical field. Our measurements were carried out for reduced temperatures above  $2 \times 10^{-3}$ . The longitudinal staggered magnetization is observed to have a very similar behavior near the antiferromagnetic to paramagnetic transition in zero field. The neutron-scattering technique can also

be used as a quantitative probe of the behavior of the *direction* of the staggered magnetization. This has been done near the spin-flop line, but with the applied field deliberately misaligned in the easy-semieasy plane by an amount large compared to the estimated angular width of the shelf of first-order spin-flop transitions. In this case, as one would expect on the basis of mean-field theory, the staggered magnetization is observed to rotate continuously as the field strength is increased through the flop value. However, on the basis of measurements made at  $\sim 0.7 T_N$ , the field span over which this rotation occurs is narrower than that predicted by mean-field theory. The magnitude of the staggered magnetization decreases by about 8% in going from the antiferromagnetic to the flopped configurations. This may be accounted for quantitatively by the anisotropy of the  $g$  factor.

#### ACKNOWLEDGMENTS

It is a pleasure to acknowledge the generous assistance of Gen Shirane during the course of this work. We are also grateful to R. J. Birgeneau, M. Blume, M. E. Fisher, C. S. Naiman, and H. Rohrer for valuable comments and discussions. Computer work at the University of Maryland supported by the Computer Science Center.

\*Work at Brookhaven performed under the auspices of the U. S. Energy Research and Development Administration.

†Present address. Work at Maryland supported by the National Science Foundation Grant No. DMR 76-81185.

‡Work at Brandeis supported by the National Science Foundation Grant No. DMR 75-03610.

§Present address: IRT Corp., P. O. Box 80817, San Diego, Calif. 92138.

<sup>1</sup>L. Néel, *Ann. Phys. (Paris)* **5**, 232 (1936).

<sup>2</sup>N. J. Poulis and G. E. G. Hardeman, *Physica (Utr.)* **18**, 201 (1952); **18**, 429 (1952).

<sup>3</sup>J. Ubbink, J. A. Poulis, H. J. Gerritsen, and C. J. Gorter, *Physica (Utr.)* **18**, 361 (1952); C. J. Gorter, *Rev. Mod. Phys.* **25**, 332 (1953).

<sup>4</sup> $\text{CuCl}_2 \cdot 2\text{H}_2\text{O}$  is orthorhombic, with the  $\vec{a}$  axis the easy magnetic direction,  $\vec{b}$  axis the next-to-easiest direction, and the  $\vec{c}$  axis the hard direction.

<sup>5</sup>J. C. A. Van der Sluijs, B. A. Zweers, and D. de Klerk, *Phys. Lett.* **24A**, 637 (1967).

<sup>6</sup>G. J. Butterworth and V. S. Zidell, *J. Appl. Phys.* **40**, 1033 (1969).

<sup>7</sup>Our "staggered magnetization" is defined such that in zero field it equals the magnetic moment of a single "up" sublattice spin [see Eq. (9)]. Strictly speaking the terminology "staggered moment per spin" might therefore be more appropriate.

<sup>8</sup>M. E. Fisher and D. R. Nelson, *Phys. Rev. Lett.* **32**, 1350 (1974).

<sup>9</sup>L. P. Kadanoff, in *Critical Phenomena, Proceedings of*

*the International School of Physics Enrico Fermi, Course LI*, edited by M. S. Green (Academic, New York, 1971).

<sup>10</sup>See the recent article by J. C. Le Guillou and J. Zinn-Justin, *Phys. Rev. Lett.* **39**, 95 (1977), and references therein.

<sup>11</sup>H. Rohrer, and H. Thomas, *J. Appl. Phys.* **40**, 1025 (1969).

<sup>12</sup>K. W. Blazey, H. Rohrer, and R. Webster, *Phys. Rev. B* **4**, 2287 (1971).

<sup>13</sup>The spin-flop bicritical point is thus a multicritical point in the temperature-field space at which the SF shelf-edge critical lines meet with the SF-P and AF-P lines, and also with the lines of transitions between the paramagnetic and "canted" states, the latter being associated with an additional strong field applied along the next-to-easiest direction. See Refs. 14 and 15 below.

<sup>14</sup>E. Domany and M. E. Fisher, *Phys. Rev. B* **15**, 3510 (1977).

<sup>15</sup>H. Rohrer and Ch. Gerber, *Phys. Rev. Lett.* **38**, 909 (1977).

<sup>16</sup>D. Harker, *Z. Kristallogr.* **93**, 136 (1936); S. W. Peterson and H. A. Levy, *J. Chem. Phys.* **26**, 220 (1957).

<sup>17</sup>G. Shirane, B. C. Frazer, and S. A. Friedberg, *Phys. Lett.* **17**, 95 (1965).

<sup>18</sup>Recall that for an orthorhombic structure the mutually orthogonal reciprocal-lattice vectors  $\vec{a}^*$ ,  $\vec{b}^*$ , and  $\vec{c}^*$  are parallel to  $\vec{a}$ ,  $\vec{b}$ , and  $\vec{c}$ , respectively. At room temperature (Ref. 19)  $a = 7.41 \text{ \AA}$ ,  $b = 8.08 \text{ \AA}$ , and

$c = 3.74 \text{ \AA}$ . At 4.2 K we obtained  $b = 8.048 \text{ \AA}$ , and  $c = 3.721 \text{ \AA}$ .

<sup>19</sup>H. Umeyashi, B. C. Frazer, D. E. Cox, and G. Shirane, *Phys. Rev.* **167**, 519 (1968). References to some of the earlier experiments and theory can be found here.

<sup>20</sup>T. Moriya and K. Yoshida, *Progr. Theor. Phys.* **9**, 663 (1953).

<sup>21</sup>W. Marshall and S. W. Lovesey, *Theory of Thermal Neutron Scattering* (Oxford U.P., New York, 1971).

<sup>22</sup>Recall that the  $\text{Cu}^{2+}$  ions have only a single magnetic electron, which combined with their low density makes extinction effects negligible. It also results in a low demagnetizing field;  $\sim 15$  Oe at an applied field of 12 kOe.

<sup>23</sup>These curves were taken at temperatures of 2.1, 3.0, and 2.8°K, respectively. For clarity the intensities were scaled so as to agree at low fields; the curves were also shifted horizontally so that all three are centered near  $H = 6700$  Oe. The actual central fields are given in Fig. 1.

<sup>24</sup>J. Skalyo, Jr., D. E. Cox, and B. C. Frazer, *Bull. Am. Phys. Soc.* **13**, 461 (1968).

<sup>25</sup>J. Van den Handel, H. M. Gijssman, and N. J. Poulis,

*Physica (Utr.)* **18**, 862 (1952).

<sup>26</sup>K. Yosida, *Progr. Theor. Phys.* **6**, 691 (1951).

<sup>27</sup>C. J. Gorter and J. Haantjes, *Physica (Utr.)* **18**, 285 (1952); N. J. Poulis and G. E. G. Hardeman, *ibid.* **20**, 7 (1954).

<sup>28</sup>T. Nagamiya, *Progr. Theor. Phys.* **11**, 309 (1954); and T. Nagamiya, K. Yosida, and R. Kubo, *Adv. Phys.* **4**, 1 (1955).

<sup>29</sup>To our knowledge this has not been remarked on previously, although this discrepancy may well appear in earlier measurements. In their study of the flop behavior at smaller misalignments ( $\psi \leq 0.2^\circ$ ) C. S. Naiman and T. R. Lawrence [*J. Appl. Phys.* **37**, 1138 (1966)] obtained apparent agreement with a theory equivalent to Eq. (14). Actually this is surprising since Eq. (14) is incorrect even in the mean-field approximation when  $\psi$  is not large compared to  $\psi_c$ . A further examination of their data [Air Force Cambridge Research Laboratories Report No. 66-16 (unpublished)] shows that for one measurement made at a larger angle the experimental width was appreciably smaller than the mean-field calculated width.

<sup>30</sup>P. Heller, *Rep. Prog. Phys.* **30**, 731 (1967).